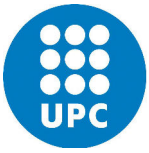

UNIVERSITAT POLITÈCNICA
DE CATALUNYA
BARCELONATECH

Erasmus
Mundus

UNIVERSITAT POLITÈCNICA DE CATALUNYA, BARCELONA

MSC. COMPUTATIONAL MECHANICS ERASMUS MUNDUS

ACADEMIC JOURNAL WRITING

Communication Skills 2

Author:
Nikhil Dave

Date: December 24, 2017

ScienceDirect
www.sciencedirect.com

Journal of Hydrodynamics, Ser. B 14 (2017) 1–6

RIAI
www.elsevier.es/RIAI

Hydrodynamic analysis of floating devices

Nikhil Dave[a], Jibran Haider[b], Dr. Fawzi Belblidia[c]

[a]*Research Assistant, MSc. Computational Mechanics, Swansea University, Bay Campus, Fabian Way, Crymlyn Burrows, Swansea, SA1 8EN, Wales, UK*
[b]*PhD Researcher, ASTUTE 2020, Swansea University, Bay Campus, Fabian Way, Crymlyn Burrows, Swansea, SA1 8EN, Wales, UK*
[c]*Senior Technical Manager, ASTUTE 2020, Swansea University, Bay Campus, Fabian Way, Crymlyn Burrows, Swansea, SA1 8EN, Wales, UK*

Abstract

We present a methodology which aims to optimise the geometric configuration of a point absorber Wave Energy Converter (WEC) to maximise the average power extraction from its intended deployment site through numerical modelling, simulation, and analysis in frequency domain. A linear frequency domain model is created to predict the behaviour of the heaving point absorber WEC system. The hydrodynamic parameters are obtained based on Boundary Element Method (BEM). A linear external damping coefficient is applied to enable power absorption, and an external spring force is introduced to tune the point absorber to the incoming wave conditions, which needs to be optimised to maximise the power extraction. Using the average annual wave energy spectrum as the input, a time domain analysis is then performed and finally we show the efficiencies of the optimised and basic shaped WEC geometries.

Received 24 December 2017 Accepted 4 January 2018

Keywords: Hydrodynamics, Wave Energy Converters, Numerical Modelling

1. Introduction

Covering over 70 percent of the Earth's surface, the oceans represent an enormous source of renewable energy. Wave energy is produced by the interaction of the wind and free surface of sea water masses [2]. Energy by the wind is transferred to water through applied shear stress and it is transported in the direction of the generated wave. This recognition of the ocean as an energy resource has been proposed as early as the late 18th century, with the first patent for harnessing the ocean's wave energy proposed by Monsieur Girard in France in 1799 [1]. Despite its promise, however, the ocean energy technology's development has staggered until the 1960s due to its high costs of construction, deployment and maintenance. Only recently, when the interest in developing new technologies for harnessing renewable energy was stimulated during the oil shortage crisis in 1973, was the ocean energy reconsidered as an alternative energy resource.

The ocean energy includes energy from waves, tides, currents and thermal gradients. The wave energy represents the largest resource of ocean energy and is capable to supply at least half of the world's electricity needs. As most forms of renewable energy sources, wave energy is unevenly distributed over the globe. An unavoidable challenge associated with wave energy is that it is harnessed offshore which increases the cost of power transfer. Therefore researchers are focusing on studying and producing more efficient ways of energy extraction from waves. Wave energy extraction is attained by the use of special devices called Wave Energy Converters (WECs).

1.1. Wave Energy Converters

The term, WEC, applies to a large variety of structures of different designs, whose aim is to turn the wave energy into electrical power. In general, the function of a WEC relies on taking advantage of the pressure variations, horizontal or vertical, produced by the varying sea surface of waves. A generator connected to the WEC device turns the produced motion into electrical power.

1.2. Point Absorber

A point absorber design (refer figure 1) is considered in the study wherein a buoy (rigid floating body) is connected to the sea bed. A Power Take Off (PTO) device is placed between the sea bed and the buoy. It aims to capture the wave-induced motion of the floater through a mechanical generator (damper) to transform it into electrical power. Additionally, the PTO device has a mechanical spring to hold the system in-line.

E-mail: n.dave@swansea.ac.uk (Nikhil Dave)
URL: www.swansea.ac.uk (Nikhil Dave)

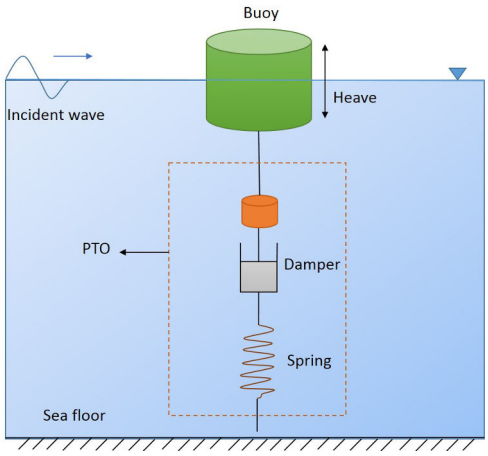

Figure 1: Basic design of a Point Absorber

1.3. Device Evaluation

Three different buoy shapes a) Vertical cylinder, b) Hemisphere - cylinder and c) Cone - cylinder are considered for the Point Absorber as shown in figure 2.

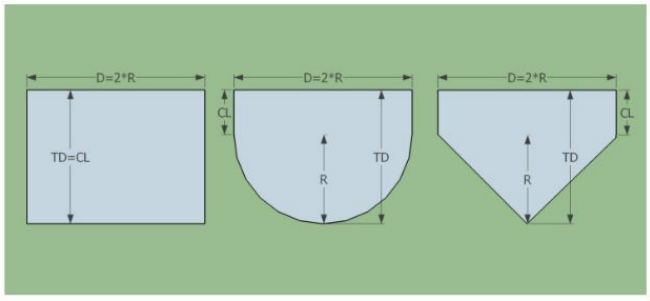

Figure 2: 2D sketch of the submerged part of the geometries considered, where: CL = the length of the cylindrical part, D = the diameter of the cylinder, R = the radius of the cylinder and TD = the total draft of the buoy

2. Basic Theory and Models

Navier-Stokes equations are generally difficult and time-consuming to solve. Hence, to facilitate the practical applicability, Linear Wave Theory (LWT), also known as potential theory, is assumed in the analysis. According to LWT, the fluid is considered as ideal and the diffusive part of equation is neglected.

$$\frac{\partial \phi}{\partial x} = u, \quad \frac{\partial \phi}{\partial y} = v, \quad \frac{\partial \phi}{\partial z} = w \tag{1}$$

2.1. Scatter Diagram

A wave rider buoy is used to measure wave conditions. The device data is used to determine significant wave height and zero up-crossing period using fourier transformation. A useful presentation of collected wave data is the scatter diagram. This shows the frequency of occurrence of sea states over a long time interval of measurements. Table 1 shows a scatter diagram considered in this analysis.

H_s [m] / T_z [s]	3.5	4.5	5.5	6.5	7.5	8.5	9.5	10.5
4.5	0	2	11	19	14	6	2	1
3.5	0	6	27	39	26	10	3	1
2.5	1	17	63	73	40	13	3	1
1.5	3	49	121	99	40	10	2	0
0.5	19	86	94	41	10	2	0	0

Table 1: Scatter diagram of the sea state

2.2. JONSWAP Wave Spectra

Fourier transformation is also applied to translate the trace of wave heights over time to a graph of power spectral density with respect to frequency, also known as the wave spectrum. The graph tells us which frequencies carried most energy in the sea during the time interval of measurements. In 1968-1969 an extensive wave measurement program, known as the Joint North Sea Wave Project (JONSWAP) was carried out along a line extending over 100 miles into the North Sea. Analysis of the data yielded a spectral formulation for fetch-limited (or coastal) wind generated seas. The definition of a JONSWAP wave spectrum [5] is given by,

$$S_\zeta(\omega) = 320 \frac{H_s^2}{T_p^4} \omega^{-5} \exp\left(\frac{-1950}{T_p^4} \omega^{-4}\right) \gamma^A \tag{2}$$

$$A = \exp\left(-\left(\frac{\frac{\omega}{\omega_p} - 1}{\sigma\sqrt{2}}\right)^2\right) \tag{3}$$

where,
$\gamma = 3.3$ = peakedness factor
σ = a step function of ω:
if $\omega \leq \omega_p$ then: $\sigma = 0.07$; if $\omega \geq \omega_p$ then: $\sigma = 0.09$
ω_p = peak frequency corresponding to the highest energy density value [rad/s]

Figure 3 depicts the energy density spectrum for a given sea state, $S_\zeta(\omega)$ plotted against the range of frequencies. The wave amplitude ζ_a can be expressed in a wave spectrum by the expression,

$$S_\zeta(\omega_n) \cdot \Delta\omega = \frac{1}{2}\zeta_{a_n}^2 \tag{4}$$

where,
$S_\zeta(\omega_n)$ = energy density corresponding to frequency ω_n $[m^2 s]$
$\Delta\omega$ = frequency interval [rad/s]
ζ_{a_n} = wave amplitude corresponding to frequency ω_n for the respective energy contribution [m]

The total energy per unit surface area of the irregular sea state is the area under the curve in the figure 3 multiplied by ρg.

$$E_{tot} = \rho \cdot g \int_0^\infty S_\zeta(\omega) d\omega \tag{5}$$

where,
E_{tot} = energy per unit sea surface area over one wave cycle $[J/m^2]$

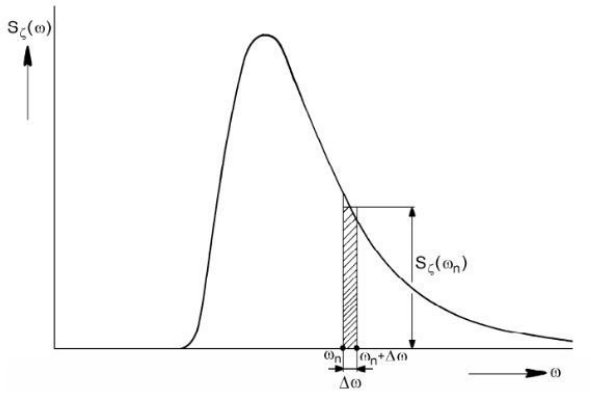

Figure 3: Definition of Spectral Density

The average power of the sea state is simply the superposition of the power of the N frequency components,

$$P_{wave} = \sum_{n=1}^{N} E_{tot_n} \cdot C_{g_n} \tag{6}$$

where,
P_{wave} = energy transfer per unit wave crest over one wave cycle [W/m]

In irregular waves, the available power over the diameter D of the point absorber [3] is expressed by,

$$P_{avail} = P_{wave}\ D \tag{7}$$

where,
P_{avail} = average available wave power over one wave cycle [W]

2.3. *Pressures and Forces*

Using Linear Wave Theory, the pressure is derived from the dispersion relationship after obtaining the total velocity potential by linear superimposition. The hydrodynamic and hydrostatic forces and moments are then determined by integration of the pressure on the submerged body surface. The equation of motion is solved for the displacement, $z(t)$ of the floating object in frequency domain.

3. Methodology

The process adopted to derive the displacement, $z(t)$ of the floating object in the frequency domain is given as,

- Deriving frequency dependent coefficients and wave excitation force using Boundary Element Method
- Solving Mass-Spring-Damper System model and deriving response amplitudes
- Calculation of the extracted power for a given geometry and sea state
- Obtaining the per sea state and average power extraction efficiency

3.1. *Frequency dependent coefficients and wave excitation force*

The frequency dependent coefficients $a(\omega)$, $b(\omega)$ and the wave excitation force amplitude, $F_{exc}(\omega)$ for the range of frequencies are calculated using the Boundary Element Method code NEMOH, developed by Ecole Centrale de Nantes. First, for a given geometry the three frequency dependent coefficients and wave excitation force are derived, as presented in Figures 4, 5 and 6 respectively. Then, on the basis of Archimedes principle and the balance between weight and buoyancy, the restoring coefficient is calculated as,

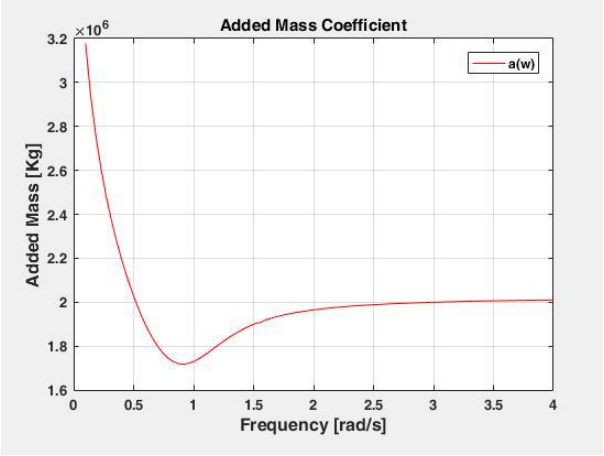

Figure 4: Added Mass Coefficient, a(w)

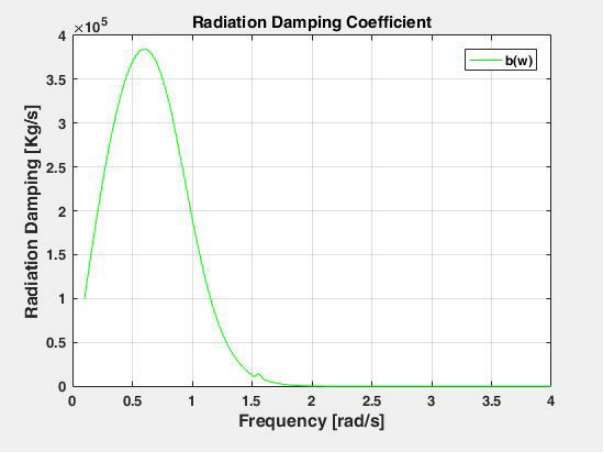

Figure 5: Radiation Damping Coefficient, b(w)

$$c = \rho g A_{wl} \tag{8}$$

where,
A_{wl} = cross-section of the buoy at water plane surface [m^2]

3.2. *Derived Response Amplitudes*

The solution of the Mass-Spring-Damper System model in the frequency domain gives the response amplitude characteristics. First we derive the mechanical spring coefficient, k_{sp} and PTO damping coefficient, β which are used in the derivation of

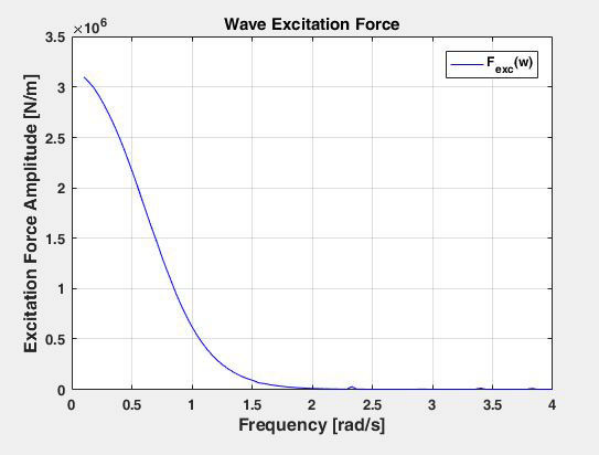

Figure 6: Wave Excitation Force, $F_{exc}(w)$

the response amplitudes. For a given wave energy spectrum, the optimum values [5] of k_{sp} and β for an irregular sea state is given as,

$$k_{sp} = \omega_p^2\,[m + a(\omega_p)] - c \tag{9}$$

$$\beta = \sqrt{b(\omega_p)^2 + \frac{1}{\omega_p^2}(-(m + a(\omega_p))\omega_p^2 + c + k_{sp})^2} \tag{10}$$

When the above equation is satisfied for a specific geometry and sea state, maximum energy absorption for peak frequency, ω_p. For a same sea state, different geometries will have a different maximum power absorption. In this research work, maximum power absorption for different geometries are compared using the same sea state.

The response amplitude characteristics are the frequency dependent ratio of the floater's response over the incoming wave amplitude. It is also referred as Response Amplitude Operator (RAO) as presented in Figure 7.

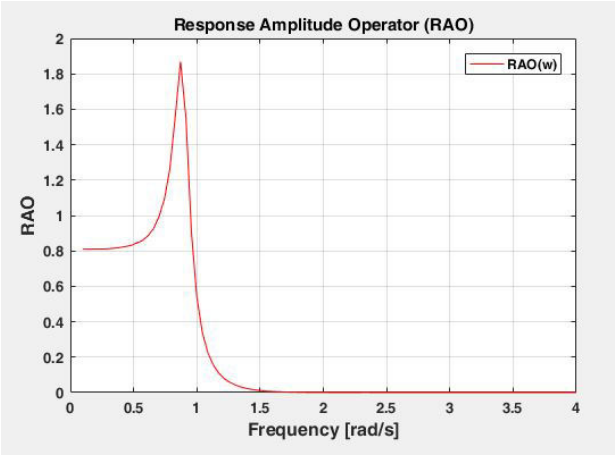

Figure 7: Response Amplitude Operator (RAO)

The mathematical description for the n^{th} frequency component of RAO [5] is given as,

$$RAO = \frac{F_{exc,a_n}(\omega_n)}{\sqrt{[c + k_{sp} - [m + a(\omega_n)] \cdot \omega_n^2]^2 + [b(\omega_n) + \beta]^2\omega_n^2}} \tag{11}$$

3.3. Extracted Power

In this section, we use the derived relations in the previous sections to calculate the average power extracted of a given geometry and sea state. As power is equal to force multiplied by velocity, we consider the PTO damping force, F_{pto} as the force generating electrical power and the required velocity is the buoy's velocity. This leads to the expression for the instantaneous power extraction [3],

$$P_{ext}(t) = F_{pto} \cdot \dot{z}(t) \tag{12}$$

By applying linear superposition of the buoy responses in N regular wave components, the power absorption in irregular waves for a given geometry [3] can be obtained by integrating equation (12) over a wave cycle using equation for the force as,

$$P_{ext} = \sum_{n=1}^{N} \frac{1}{2} \cdot \beta(\omega_n) \cdot \omega_n^2 \cdot RAO(\omega_n) \cdot \zeta_{a_n}^2 \tag{13}$$

The number of the frequency components, N depends on the frequency grid resolution and the range of frequencies accounted. In the present analysis, a frequency grid convergence study is performed in section 4.1 to determine the optimum number of frequency components.

3.4. Efficiency

As mentioned earlier, the wave energy transfer occurs in the direction of wave propagation. This means that buoys of larger radii will have access to larger amounts of wave energy. On the other hand, over dimensioning the buoy will increase its mass and can subsequently lead to increase in the buoy's inertia forces. This will eventually decrease its velocity and extracted wave energy. Therefore, although a larger buoy absorbs more wave energy, it is not as efficient as the smaller one since its absorption efficiency is smaller. Hence, in the present analysis, the dimensionless quantity, Efficiency is used to evaluate different designs with the same available wave energy, by keeping the same diameter of the buoy shape. The extraction efficiency, or briefly efficiency, denoted by η, is defined as the ratio of the average extracted power to the average available power [3] and is given as,

$$\eta = \frac{\bar{P}_{ext}}{\bar{P}_{avail}} \tag{14}$$

The average extracted and the average available power are evaluated by taking an average over the sea states in the scatter diagram weighted with the number of occurrences annually.

4. Results and Discussion

4.1. Frequency step convergence study

The frequency domain model and BEM code, NEMOH are employed for comparing the effect of frequency step size or

the number of frequencies for the model. The frequency range being used in this study is set to 0.1 - 4.0 rad/s. The effect of frequency step size/interval, $\Delta\omega$ on the average available power and average extracted power over the scatter diagram was studied for $\Delta\omega$ = 0.1, 0.01 and 0.001 rad/s and Figure 8 and 9 show the results, The number of panels (mesh size) used for mesh-

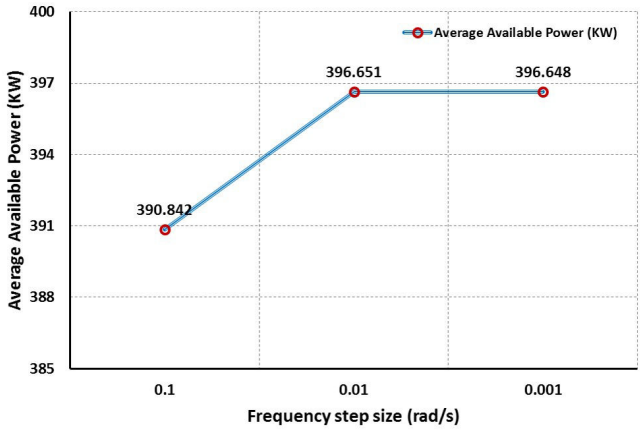

Figure 8: Average available power convergence based on frequency step size

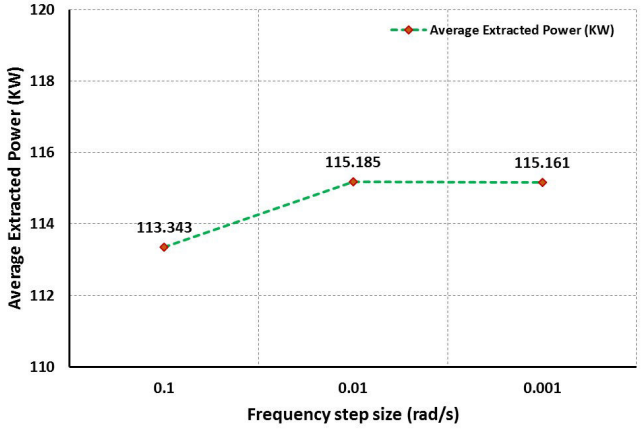

Figure 9: Average extracted power convergence based on frequency step size

ing was constant and set to 1562 panels for varying frequency step size. It can be inferred from the study that the difference between the results for frequency interval, $\Delta\omega$ = 0.01 rad/s and $\Delta\omega$ = 0.001 rad/s is considerably less. Therefore, based on the frequency step convergence study, it was decided to use $\Delta\omega$ = 0.01 rad/s as the standard frequency step size for all further simulations.

4.2. Grid Independence Study (GIS)

Carrying out grid independence tests is vital in determining the precision of numerical results. It is used to describe an improvement of results by using successfully smaller grid sizes until they become grid independent. Six grid sizes were studied, with number of mesh panels varying from 294 to 4411. Figure 10 shows the results obtained. A comparison of the average extracted power for different number of mesh panels is shown since the available wave power only depends on the sea data and the diameter of the buoy. We can easily deduce from the figure 10 that the difference between the results obtained by using 1562 and 4411 mesh panels is significantly less. Therefore it was decided to use 1562 panels as the standard mesh for further analysis.

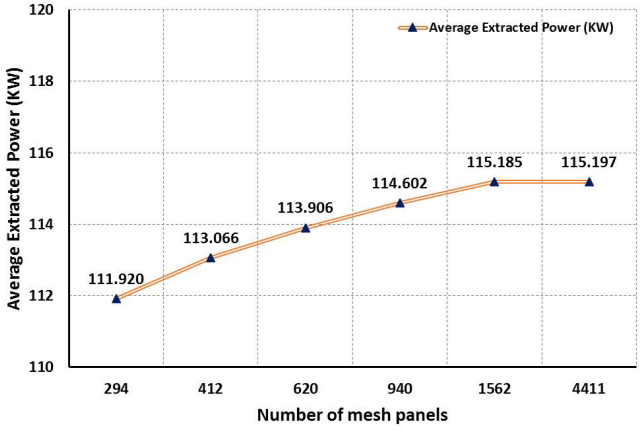

Figure 10: Average extracted power convergence - Grid Independence Study

4.3. Available Power, P_{avail} per sea state

Figure 11 shows the plot for the results obtained for the available power, P_{avail} per sea state. Based on the scatter diagram in table 1, the contribution of every sea state to the average available power is given in Table 2. The area marked in the table 2, at sea states with T_z = 5.5s, T_z = 6.5s and T_z = 7.5s represents 80% of the average available power. Also, classification of sea states with T_z shows us that the sea states with T_z = 6.5s have the most energy.

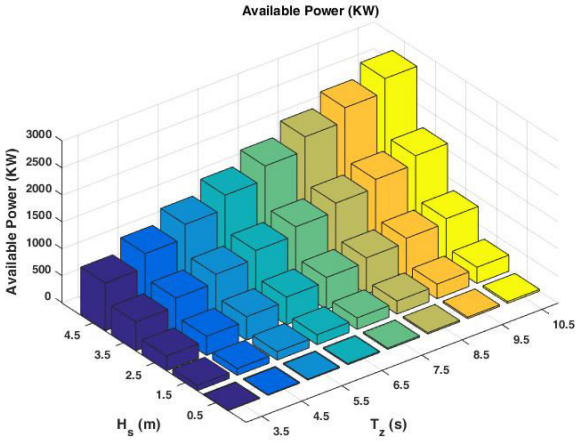

Figure 11: Plot for Available power P_{avail} per sea state [kW]

H_s [m] / T_z [s]	3.5	4.5	5.5	6.5	7.5	8.5	9.5	10.5
4.5	0	2.404	16.2	33.1	28.16	13.68	5.097	2.817
3.5	0	4.363	24.05	41.1	31.63	13.79	4.625	1.704
2.5	0.286	6.307	28.64	39.25	24.83	9.147	2.36	0.869
1.5	0.309	6.544	19.8	19.16	8.938	2.533	0.566	0
0.5	0.218	1.276	1.709	0.882	0.248	0.056	0	0

Table 2: Contribution of every sea state to the average available power, $\bar{P}_{avail}$ [kW]

4.4. Average available power, $\bar{P}_{avail}$

The average available power, $\bar{P}_{avail}$ is derived by assessing all the sea states of the scatter diagram and is presented in table 3. Since, the average available power is proportional to the design radius, R, the three considered buoy shapes - vertical cylinder, hemisphere-cylinder and cone-cylinder have access to the same available wave power.

Cylinder			
Radius [m]	Mesh panels	Frequency step [rad/s]	Avg. P_{avail} [KW]
10	1562	0.01	**396.65**

Table 3: Average available power,$\bar{P}_{avail}$ [kW]

4.5. Extracted power, P_{ext} per sea state and average extracted power, $\bar{P}_{ext}$

The contribution of every sea state to the average extracted power based on the scatter diagram, is computed. It was noted that sea states with T_z = 5.5s, T_z = 6.5s and T_z = 7.5s represents 79% of the average extracted power wherein sea states with T_z = 6.5s contribute the most. Table 4 shows the average extracted power, $\bar{P}_{ext}$, derived by assessing all the sea states of the scatter diagram.

Cylinder			
Radius [m]	Mesh panels	Frequency step [rad/s]	Avg. P_{ext} [KW]
10	1562	0.01	**115.19**

Table 4: Average extracted power,$\bar{P}_{ext}$ [kW]

4.6. Efficiency per sea state and average efficiency, η

Figure 12 shows a surface plot for the efficiency per sea state. The results shows that the design has better efficiency for sea states with $T_z \geq 5.5$s compared to $T_z \leq 4.5$s. The average efficiency, η derived by assessing all the sea states of the scatter diagram is shown in Table 5. All the results obtained for

Cylinder			
Radius [m]	Mesh panels	Frequency step [rad/s]	Avg. Efficiency (Ƞ)
10	1562	0.01	**0.2904**

Table 5: Average Efficiency, η

the cylindrical shaped buoy from the frequency domain analysis are in agreement with the numerical results obtained in the published research work by Backer et al. [3], Goggins / Finnegan [6], Pastor / Liu [4] and Kalofotias [7]. The accuracy of the developed frequency domain analysis method was therefore validated. Similar study was performed for the other two shapes: hemisphere-cylinder and cone-cylinder. The buoys of same diameter and same draft from the water line were analysed and it was concluded that the power extraction capacity of the cone-cylinder shaped buoy was slightly better than the hemisphere-cylinder shaped buoy.

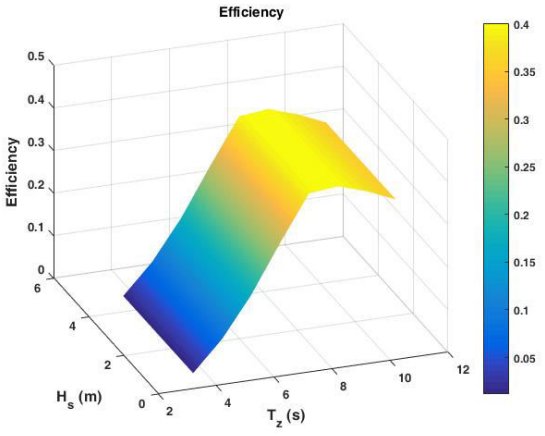

Figure 12: Plot for Efficiency per sea state

5. Conclusion

Wave energy converters (WECs) have been developed as a means to extract energy from the sea and generate electricity from a renewable source.The scope of this research work was to develop a simulation model to investigate the power extraction efficiency of a heaving buoy connected to the seabed with a spring and a linear damper system. This model could then be used to investigate buoy behaviour in different wave conditions. The power extraction efficiency of three shapes were compared and it was inferred that the cone-cylinder shape performs better than the other two shapes. A validation of the results was provided with the previous published work. Furthermore, the verification of the simulation model against experimental results would provide a greater overall confidence in the research.

References

[1] NREL, 2009. Ocean Energy Technology Overview. U.S. National Renewable Energy Laboratory 135, 7–9 DOE/GO-102009-2823, July 2009
[2] Electrical Power Research Institute, EPRI, (2005), Ocean Tidal and Wave Energy Renewable Energy Technical Assessment GuideaTAG-RE
[3] Griet De Backer, Hydrodynamic Design Optimization of Wave Energy Converters Consisting of Heaving Point Absorbers. Ghent University, Belgium, 2009
[4] Jeremiah Pastor, Yucheng Liu, Frequency and time domain modeling and power output for a heaving point absorber wave energy converter Int J Energy Environ Eng (2014) 5:101DOI 10.1007/s40095-014-0101-9
[5] J.M.J. Journée and W .W. Massie. Offshore hydromechanics January. 2001. doi: 10.1016/S0013-4686(01)00879-9
[6] Jamie Goggins, William Finnegan, Shape optimisation of floating wave energy converters for a specified wave energy spectrum Renewable Energy 71 (2014) 208-220
[7] Filippos Kalofotias, Study for the Hull Shape of a Wave Energy Converter-Point Absorber, University of Twente, 2016